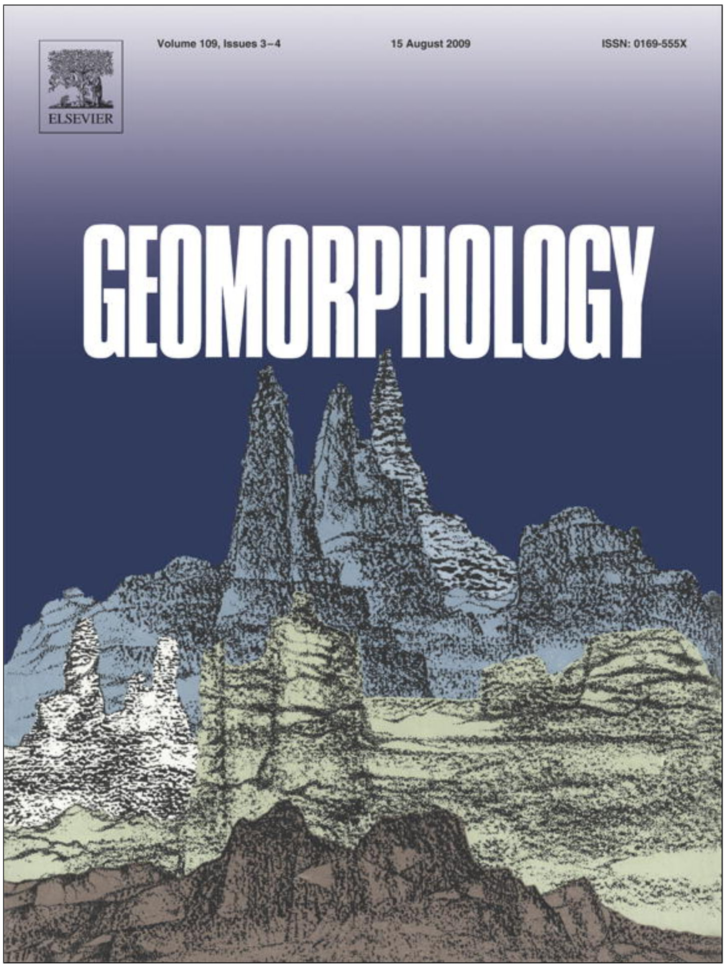
Volume 109, Issues 3–4
15 August 2009
ISSN: 0169-555X
ELSEVIER
GEOMORPHOLOGY

Geomorphology 109 (2009) 184–196

Contents lists available at ScienceDirect

Geomorphology

journal homepage: www.elsevier.com/locate/geomorph

Morphology and structure of a landslide complex in an active margin setting: The Waitawhiti complex, North Island, New Zealand

Aurélien Lacoste [a,*], Lies Loncke [b], Frank Chanier [a], Julien Bailleul [c], Bruno C. Vendeville [a], Geoffroy Mahieux [d]

[a] UMR 8157 Géosystèmes, Université de Lille 1, Bâtiment SN5, 59655 Villeneuve d'Ascq Cedex, France
[b] Université de Perpignan, Via Domitia, Laboratoire IMAGES, Bat U, 2e étage, 52 avenue Paul Alduy, 66800 Perpignan, France
[c] Institut polytechnique Lasalle-Beauvais, Département Géosciences, 19 rue Pierre Wagner, 60000 Beauvais, France
[d] Université de Picardie Jules Verne, 33 rue St-Leu, 80000 Amiens, France

ARTICLE INFO

Article history:
Received 4 August 2008
Received in revised form 2 March 2009
Accepted 3 March 2009
Available online 14 March 2009

Keywords:
Landslides
New Zealand
River incision
Gas seeps
Tectonics

ABSTRACT

Multi-scale gravitational instabilities are widespread in the Coastal Ranges of the North Island of New Zealand. We document here a detailed analysis of the Waitawhiti landslide complex, located in the core of the Tawhero syncline, and investigate the potential landslides triggering factors in the area. Four contiguous large slides form the Waitawhiti complex. These slides involve fine-grained Miocene sandstones and massive fractured siltstones. Sliding occurs mostly along nearly horizontal strata. All slides are bounded laterally and/or distally by deep-incised valleys. Three gas seeps evidencing thermogenic gas release have been discovered in the vicinity of the slides. We propose that river incision, continuously removing distal buttresses, is the main destabilizing factor in the area. However, additional factors, such as tectonic activity and intense rainfall, cannot be excluded. We also propose that fluid overpressure, reducing the effective shear strength at the base of low-permeability layers, may have influenced the triggering of landslides in the Waitawhiti area.

1. Introduction

Landsliding is an erosional process contributing to the denudation of mountain ranges in active margin settings (Hovius et al., 1997; Lin et al., 2006; Meng et al., 2006). It is likely that intense landsliding greatly accelerates mountain denudation. Although its relative contribution is obviously important, it is often difficult to assess in mass balances terms. Investigations into the occurrence and conditions allowing landsliding are thus important in these situations. The study of landslides also has an important human dimension because of the hazards associated with landslides.

Determining factors, such as surface-uplift rates or weak lithologies, coupled with external factors, usually cause mass movements along hillslopes. Two main external triggering factors are commonly identified: (1) intense rainfall that leads to increased pore-fluid pressure, hence to reduced shear strength (Rogers and Selby, 1980; Chen et al., 2006), and (2) earthquakes, that are also considered as a major destabilizing factor (Keefer, 1984; Crozier et al., 1995; Chang et al., 2005).

The Hikurangi margin, located east of the North Island of New Zealand, is an active margin that formed during westward subduction of the Pacific plate. The inner part of its accretionary prism emerges and is affected by many gravitational instabilities at various scales, ranging from shallow soil slips (Pearce et al., 1987) to crustal-scale gravitational collapse (Pettinga, 2004). Shallow slips or earthflows generally result from intense rainfall coupled with the lack of vegetation cover induced by massive deforestation (Pearce et al., 1987; Zhang et al., 1993; Reid and Page, 2002). Conversely, some of the largest instabilities have been correlated with high-magnitude historical earthquakes (e.g., landslide volume up to 72×10^6 m^3: the Napier 1931 earthquake; Hancox et al., 1997). Some deep-seated landslides even reflect regional extension and are associated, depending on the sites, with gravitational collapse caused by tectonic underplating (Barnes and Lewis, 1991; Chanier et al., 1999; Pettinga, 2004).

The Coastal Ranges of the eastern North Island of New Zealand are presently subjected to high surface-uplift rates, up to 2.3 mm yr^{-1} (based on marine terraces elevations; Ghani, 1978; Pillans, 1986; England and Molnar, 1990), and are the locus of numerous gravitational instabilities. Using satellite imagery and field work analysis, we document the distribution and morphology of a cluster of gravitational instabilities (average surface of each landslide is 1 km^2) within a selected area of the Coastal Ranges (Tawhero syncline). Our goal is to precisely delineate and characterize the relationship between the onset of landslides and the different internal and external geologic parameters of the area, such as climate, tectonics, lithology, and pore fluids.

2. Geological setting of the Waitawhiti complex

2.1. Geodynamics

The North Island of New Zealand is located on the upper plate of the Hikurangi subduction zone, at the southern end of the Tonga–Kermadec

* Corresponding author. Tel.: +33 3 20434692; fax: +33 3 20434910.
E-mail address: aurelien.lacoste@ed.univ-lille1.fr (A. Lacoste).

0169-555X/$ – see front matter
doi:10.1016/j.geomorph.2009.03.001

subduction (Fig. 1a). Rates of subduction range from 41 mm yr^{-1} in the South to 47 mm yr^{-1} in the North of the Hikurangi trough (Fig. 1a; De Mets et al., 1994).

The Hikurangi margin comprises three major structural elements (Fig. 1b) between the Hikurangi trough and the volcanic arc (Taupo Volcanic Zone, Fig. 1b). (1) The subduction wedge, whose highest ridges are up to 1000 m high, emerge and correspond to the Coastal Ranges (Spörli, 1980), (2) the forearc basin (Ballance, 1993), 10 to 30 km-wide and (3) the Axial Ranges. The Waitawhiti complex belongs to the Coastal Ranges domain.

Owing to crustal-scale partitioning, the oblique subduction is accommodated in the Coastal Ranges by two fault families, reverse faults and right-lateral faults, as has been described in a variety of other subduction zones (e.g., Indonesia and the Philippines; Fitch, 1972; Yu et al., 1993; McCaffrey et al., 2000). The Coastal Ranges are subjected to intense seismic activity. Since the 19th century, at least fifteen earthquakes of magnitude $M>6$ have occurred in the area (www.geonet.org.nz; Hull, 1990; Schermer et al., 1998; Rodgers and Little, 2006). Within a 45-km range of the study area, four major historical earthquakes have been recorded (Fig. 2): Pahiatua 1934 ($M_W=7.4$; Schermer et al., 1998), Weber II 1990 ($M_L=6.4$; Louie et al., 2002), and two events in the Dannevirke area (1989, $Ms=6.3$ and 1990, $Ms=6.7$; www.ngdc.noaa.gov). These large earthquakes have been attributed to slip along right-lateral or right-lateral transpressional faults (e.g., the Alfredton, Saunders Road and Waitawhiti faults; Lee and Begg, 2002; Schermer et al., 2004).

2.2. Presence of fluid ascents along the Coastal Ranges

Along active margins, the influence of pore fluids on deformation has been emphasized by many authors (e.g., Henry and Le Pichon, 1991). In these settings, overpressured fluids commonly escape to the surface, forming gas seeps and mud volcanoes. Such seeps and associated mud volcanoes are found in the study area (Johnston, 1975) and all along the Coastal Ranges (Lillie, 1953; Kvenvolden and Pettinga, 1989; Francis, 1995; Pettinga, 2003). Methane is the predominant gas in the seeps, and is often associated with the generation of hydrocarbons at depth (Kvenvolden and Pettinga, 1989; Francis, 1995). Isotope studies show that the seeps have a thermogenic origin (Francis, 1995). The depth of generation of the gas is difficult to determine precisely, but Pettinga (2003) estimated it to be less than 6.5 km. These fluids often migrate upward through fault zones, especially along strike-slip faults (Chanier, 1990; Pettinga, 2003). The presence of fluids generated at depth can be an important parameter to take in account when studying landslides because these fluids may be accumulated below shallow low-permeability strata, therefore reducing the effective rock strength and triggering gravitational slides (e.g., Storegga slide, Huhnerbach and Masson, 2004; Amazon deep-sea fan, Cobbold et al., 2004).

2.3. Geology

The high number of multidirectional slides we identified, along with their clear surface expression, makes the Waitawhiti landslide

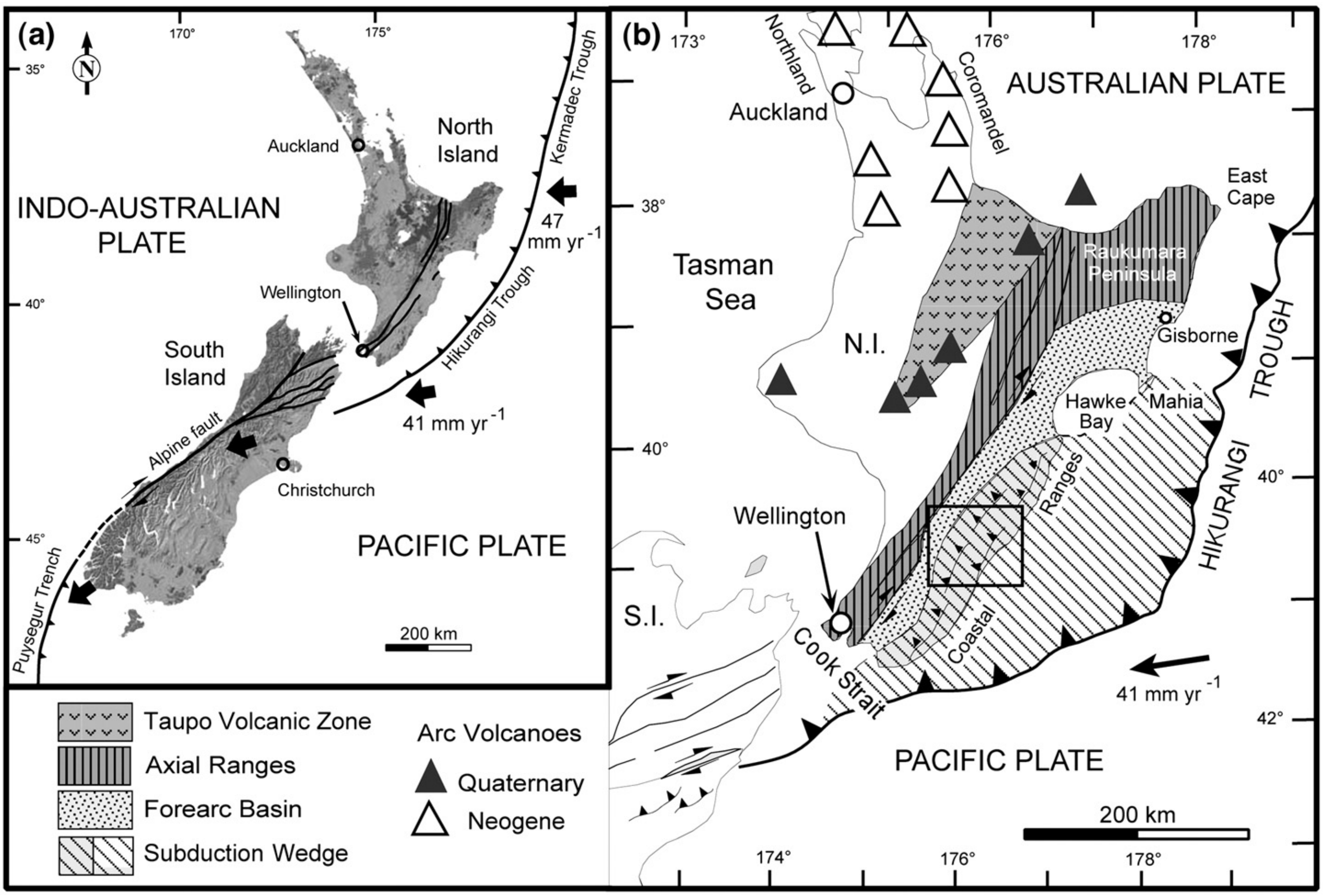

Fig. 1. New Zealand geodynamics. (a) Tectonic setting of New Zealand. (b) Main morphostructural features of the North Island of New Zealand. Black arrows show the present-day relative plate motion between the Pacific and Australian plates. Location of Fig. 2 is indicated by the inset box. N.I.: North Island; S.I.: South Island. Modified after Chanier et al. (1999).

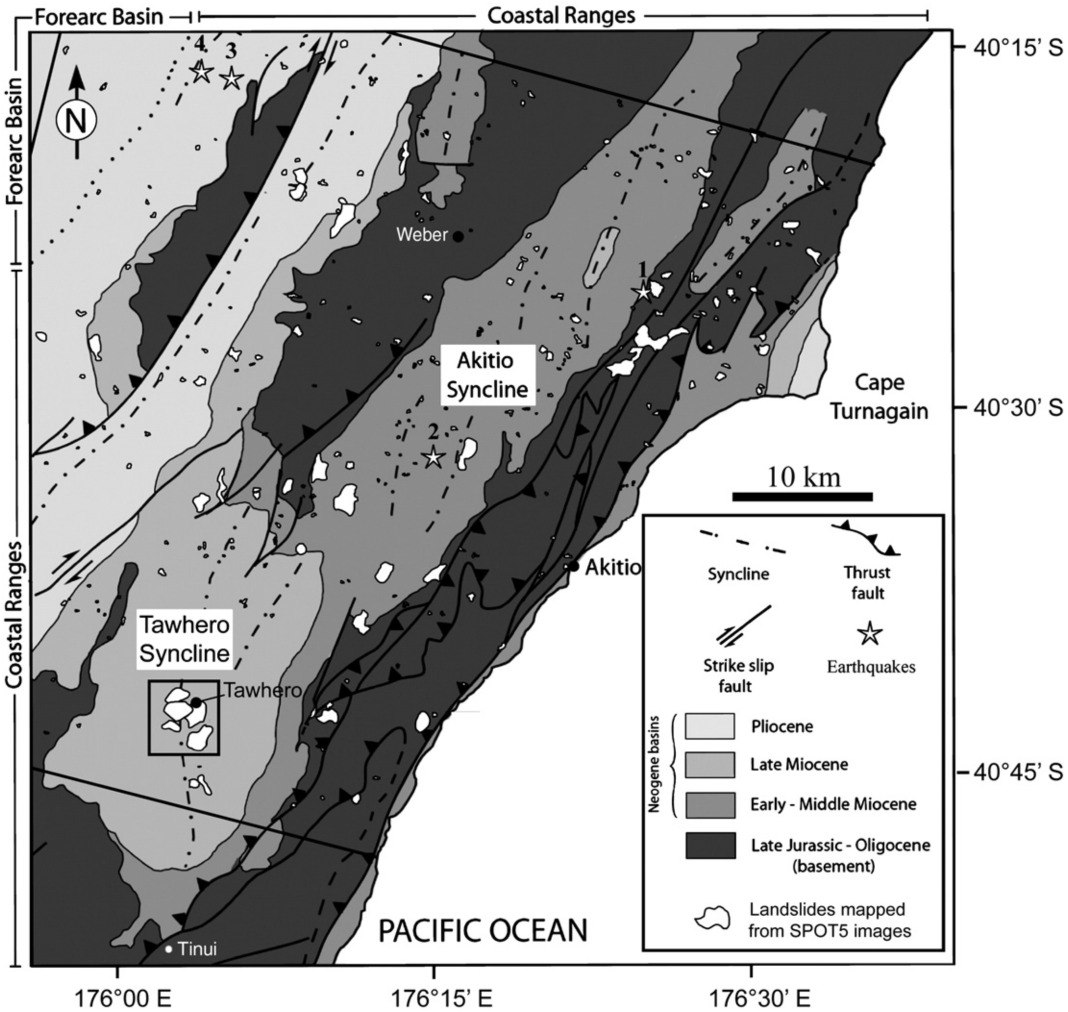

Fig. 2. Simplified geological map (location in Fig. 1) and large landslide distribution in the Cape Turnagain area (modified after Lee and Begg, 2002). Stars indicate the epicentres of major earthquakes. 1: Weber II 1990 (M_L = 6.4); 2: Pahiatua 1934 (M_W = 7.4); 3: Dannevirke 1989 (Ms = 6.3); 4: Dannevirke 1990 (Ms = 6.7). Straight black lines indicate SPOT5 image extent. Location of Fig. 3 is indicated by the inset box.

complex, located 50 km southwest of Cape Turnagain (Fig. 2), one of the largest and most intriguing landslide cluster in the North Wairarapa region. The complex is located in the core of a large open syncline, the Tawhero syncline (Johnston, 1975; Neef, 1992; Bailleul et al., 2007). The syncline (Fig. 2) is one of the major compressional structures trending parallel to the margin (Neef, 1992; Bailleul et al., 2007). Rapid uplift during the Quaternary in the area has led to emersion and good outcropping conditions of thick turbiditic sequences in the Tawhero and Akitio synclines (Fig. 2; Bailleul et al., 2007). These sequences have been interpreted as deposits of trench–slope basins (Neef, 1992; Bailleul et al., 2007). The Tawhero syncline comprises series of late Miocene age, ranging from ca. 13.2 to 5.3 Ma, overlying Mesozoic basement rocks (Bailleul, 2005). The sediments affected by landslides in the axis of the syncline are of late Tongaporutuan (ca. 9–6.5 Ma) to Kapitean (ca. 6.5–5.3 Ma) ages (Lee and Begg, 2002).

2.4. Climate and vegetation

The climate in the study area is temperate, having moderate temperatures (14 °C annual average) and rainfall (1200 mm yr^{-1} since 1970, www.niwa.co.nz). However, the East Coast can be exposed to tropical cyclonic events ("Giselle" in 1968 and "Bola" in 1988). The Coastal Ranges, and New Zealand as a whole, have been massively deforested with the first arrival of Polynesian settlers 1000 years ago and that of Europeans settlers since 1840. Increasing farming activity since the beginning of the 20th century has led to the destruction of more than 80% of the forests along hillslopes, now covered mainly with grass, and undergoing important erosion during seasonal rainfall.

3. Methodology

3.1. Morphostructural analysis

We acquired two stereoscopic panchromatic SPOT5 images in 2005 (acquisition sponsored by the French ISIS program). These images cover a 60-km^2 area in the central Coastal Ranges (northern Wairarapa region, Fig. 2). The images have a resolution of 5 m per pixel and can reach a 2.5 m resolution when associated using stereoscopy. They were geometrically rectified and spatially geo-referenced using the GEO-image software; then radiometrically improved. We conducted a detailed interpretation of these images and identified the main landscape features such as structural lineaments, fault traces and

Fig. 3. Morphostructural map of the Waitawhiti landslide complex as deduced from the analysis of SPOT5 and Quickbird images. (a) Ortho-rectified Quickbird image. (b) Morphostructural map. See location in Fig. 2. Black lines indicate location of cross sections A and B (see Fig. 5).

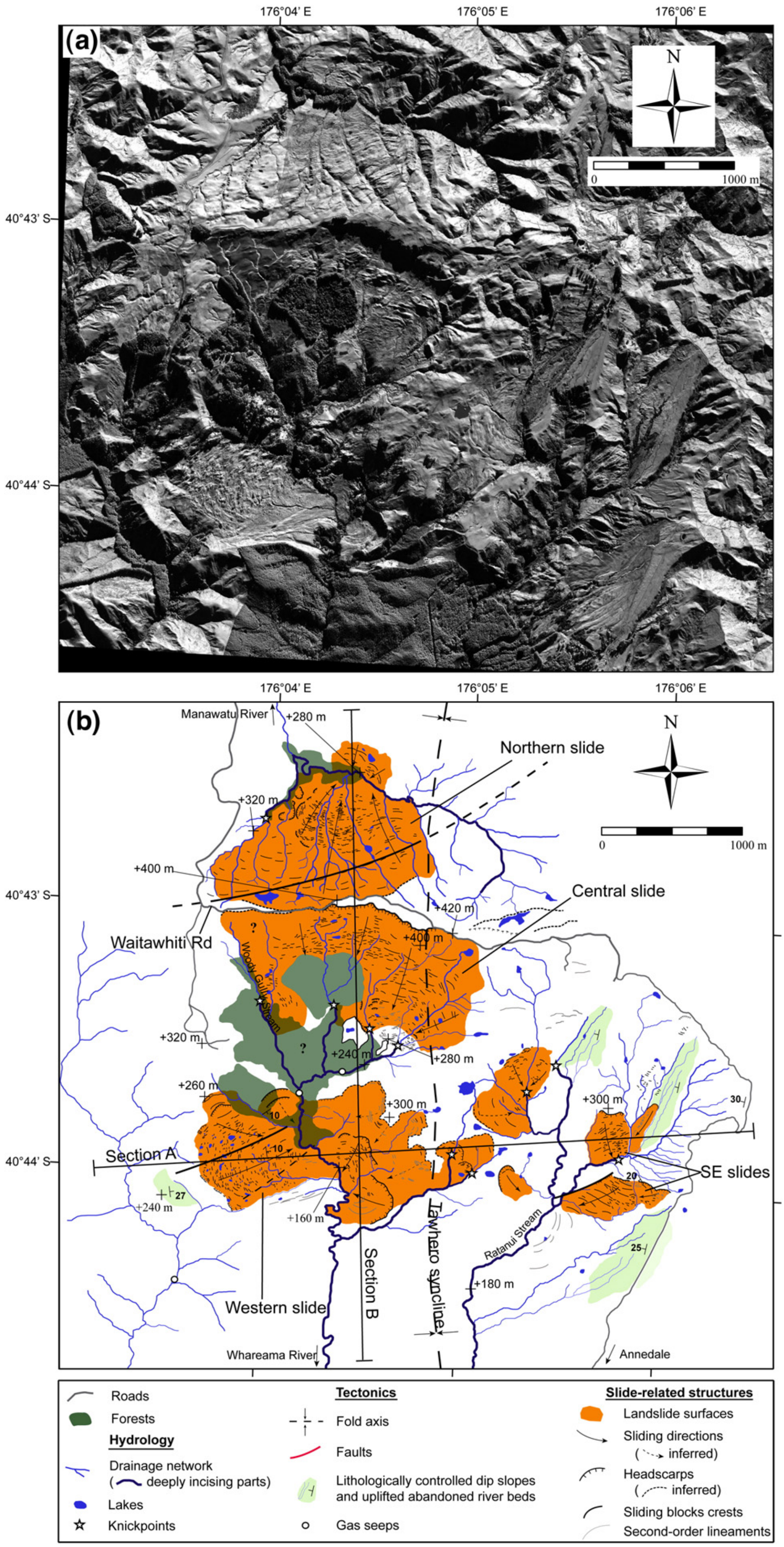

176°04' E
176°05' E
176°06' E
40°43' S
40°44' S
(a)
N
0
1000 m
(b)
Manawatu River
+280 m
+320 m
+400 m
Northern slide
Central slide
+420 m
+400 m
Waitawhiti Rd
Woody Gully Stream
+320 m
+240 m
+280 m
+260 m
+300 m
+300 m
30
10
10
Section A
27
+240 m
+160 m
20
SE slides
25
Ratanui Stream
Tawhero syncline
Section B
+180 m
Western slide
Whareama River
Annedale
Roads
Forests
Hydrology
Drainage network
(deeply incising parts)
Lakes
Knickpoints
Tectonics
Fold axis
Faults
Lithologically controlled dip slopes and uplifted abandoned river beds
Gas seeps
Slide-related structures
Landslide surfaces
Sliding directions
(inferred)
Headscarps
(inferred)
Sliding blocks crests
Second-order lineaments

landslides. This allowed us to map a thousand slides and discover clusters of landslides along a great part of the Coastal Ranges (Fig. 2). We compiled our observations in a GIS database using the ArcMap software. We also integrated bibliographic data to this database, such as the location of gas seeps (Johnston, 1975; Field et al., 1997), epicentres of historical earthquakes (www.geonet.org.nz), uplift rates (Pillans, 1986) and lithological formations and structures from geological maps (Johnston, 1975; Lee and Begg, 2002). We then analysed three Quickbird images (resolution 0.6 m per pixel, acquired in 2003, 2006 and 2008) focusing on the Waitawhiti landslide complex, which appeared to be one of the largest and best expressed landslide cluster we could identify on SPOT5 images. Through field work in the area, we calibrated the satellite observations, improved the local mapping, and analyzed in detail the structure and lithology of the identified landslides (Fig. 3).

3.2. Grain-size analyses and clay mineralogy

We conducted grain-size analyses on rocks of the study area using the principle of diffraction and diffusion of a monochromatic laser beam on suspended particles. This method is based on near-forward scattering of a laser beam by particles in suspension (Loizeau et al., 1994). The composition of clay mineral assemblages was determined following the protocol of Bout-Roumazeilles et al. (1999).

4. Results

4.1. Main presentation of the sliding complex

We analysed a total of four landslides within the Waitawhiti landslide complex (Fig. 3): the northern, central, western and southeastern Waitawhiti slides, respectively. The Waitawhiti landslide complex has a cumulated sliding area of 3.71×10^6 m^2. Individual sliding areas are in the order of 1 km^2 (Fig. 3). The total volume of displaced material is estimated to be 111×10^6 m^3. Sliding occurs or occurred at different elevations in the area (Fig. 3). The northern and central slide elevations range from 280 to 420 m above sea level (a.s.l.), whereas those of the western slide range from 160 to 260 m. Sliding directions can be either parallel (northern and central slides) or perpendicular (western slide) to the Tawhero syncline axis (Fig. 3). From SPOT5 and Quickbird satellite images, we observe that the slides have a roughly triangular shape (Fig. 3), wide upslope and narrowing downslope. River incisions are deep in the study area, especially downstream of the knickpoints we could observe (Fig. 3). Within the slides, we identified numerous sliding blocks having crests trending perpendicular to the sliding direction (Fig. 3). These blocks vary in size, with heights up to 20 m. Peat-bogs often form in the depressions at the foot of the sliding blocks. By radiocarbon dating the organic matter trapped in these peat-bogs, we were able to estimate minimum ages for the slides (Lang et al., 1999), as presented in Section 4.5.

Three active faults crossing or bounding the northern, western and southeastern slides attest of recent tectonic activity (Fig. 3). These faults strike east–northeast to northeast. This trend, parallel to the margin direction, is consistent with the regional trend of right-lateral active faults in the Coastal Ranges (e.g., the Carterton and Waitawhiti faults; Lee and Begg, 2002; Schermer et al., 2004). The presence of abandoned uplifted river beds observed along the eastern flank of the Tawhero syncline also indicates ongoing compressional deformation in the study area (Fig. 3).

4.2. Stratigraphy and fluid seeps in the stable domains

We established a synthetic lithostratigraphic column of the upper Tongaporutuan and Kapitean in the Waitawhiti area (Fig. 4). Three members, having different petrophysical characteristics, have been defined within these turbiditic sequences (Fig. 4; Bailleul, 2005; this study). Units A, B1 and B2 form an upward-coarsening sequence and Unit C shows an upward-fining sequence.

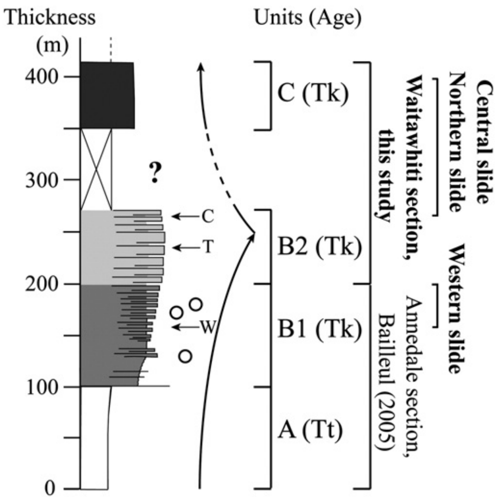

Fig. 4. Synthetic sedimentological section in the stable domains in the Waitawhiti area. Arrows indicate approximate positions of the *décollement* planes. W: western slide *décollement* plane; C: central slide *décollement* plane; T: tephra layer. White circles indicate approximate positions of the identified gas seeps. Tt: Tongaporutuan (ca. 9–6.5 Ma); Tk: Kapitean (ca. 6.5–5.3 Ma).

Bailleul (2005) demonstrated that Units A, B1 and B2 are a prograding sequence. The base of this sequence (Units A and B1) crops out in the Annedale region, 3 km south of the Waitawhiti landslide complex. The fine mud-rich turbiditic successions of Unit B1, interpreted to reflect a bathyal (>600 m depth; Bailleul, 2005) depositional environment, evolve into the lobe-facies (Bailleul, 2005) sand-rich turbidites of Unit B2 (Fig. 4). In the study area, the top of Unit B2 shows progressive decreasing thicknesses of the sandstone beds. Unit C is made of massive weathered siltstone with nodules (Fig. 4). The contact between Unit B2 and Unit C could not be observed in the field because of the slides (Fig. 5).

Grain-size analyses revealed that sandstones of Units B1 and B2 are fine-grained sandstones, having at least 49% of the grains ranging between 2 and 63 µm in size (Table 1). Siltstone layers of Units B1, B2 and C show pervasive concentric fractures, typical of spheroidal weathering processes (Sarracino and Prasad, 1989). The siltstones comprise at least 89% of grains whose sizes range between 2 and 63 µm (Table 1). Some siltstone layers have high clay contents, up to 18.8% of grains <4 µm in size (Table 1). X-ray diffraction measurements revealed that, when present, the clay content is largely dominated by smectite (up to 75%, Table 1). At the base of the western, northern and central slides, we identified such smectite-rich layers (Fig. 4, see discussion below). We have also detected one tephra layer, within Unit B2 (Fig. 4), in the southeastern slide area. This layer, overlain by the sliding mass (Fig. 5), has a low clay content (~6%), once again dominated by smectite (Table 1). When water-saturated, tuffaceous rocks like this one commonly act as landslides shear surfaces (Shuzui, 2001).

Deep thermogenic fluid seeps have been previously described 5 km southwest of the study area (Johnston, 1975). Field work allowed us to identify three new gas seeps within the Waitawhiti landslide complex; two of them located in a stream south of the central slide, and one located south of the western slide (Figs. 3, 4 and 5). Intermittent bubbling water evidences the ascent of methane gas to the surface (Fig. 6). Iridescence phenomena in stagnant water near the seeps attest of the presence of hydrocarbons in the fluids. Thus, these fluids probably are of thermogenic origin, as those described by Kvenvolden and Pettinga (1989), Francis (1995) and Pettinga (2003). The fact that all three gas seeps are stratigraphically located in Unit B1 only (Fig. 4), regardless of their geographic elevation, suggests that lateral gas migration took place within the highly permeable sandstone layers.

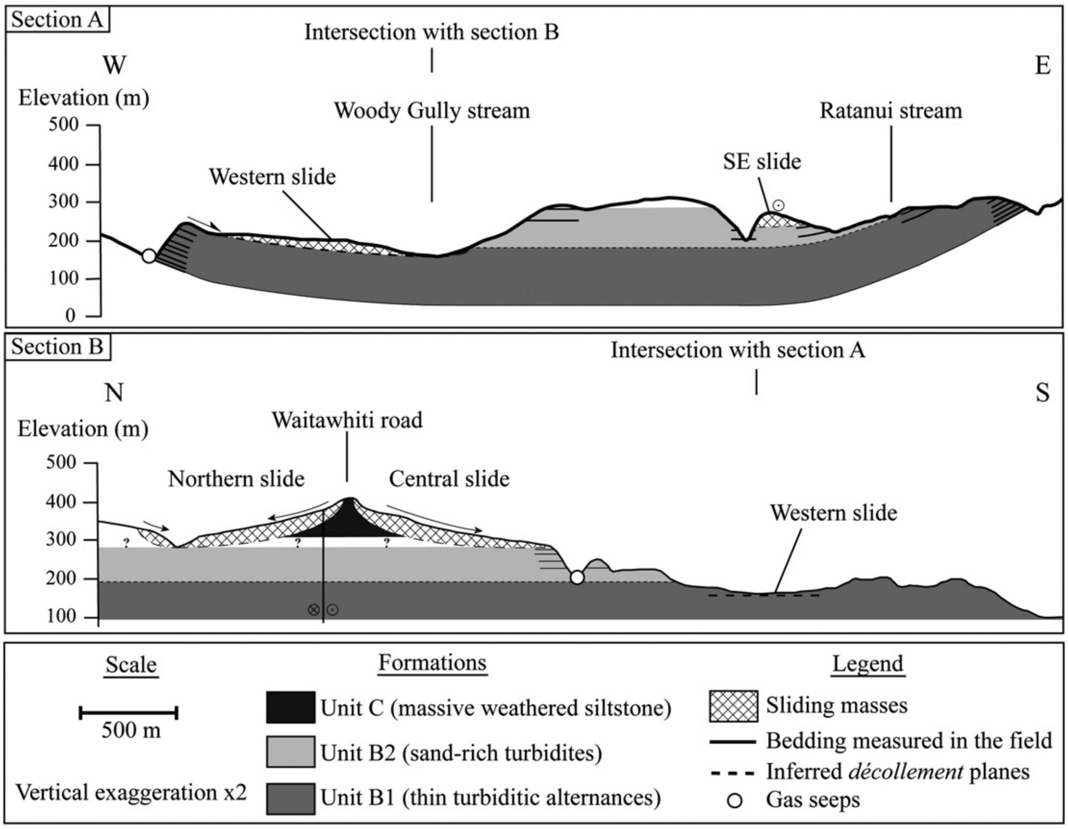

Fig. 5. Cross sections across the Waitawhiti landslide complex. Arrows indicate sliding directions. See locations in Fig. 3.

4.3. Geotechnical elements

We performed uniaxial compression tests on sandstone and siltstone samples from the study area in order to estimate the overall strength of these rocks. Two different sandstone and siltstone samples were tested under different conditions of ambient relative humidity (Fig. 7). Siltstone samples appear to be about six times more resistant than sandstone samples (Fig. 7). Also, the strength decreases linearly

Table 1
Grain-size analysis and clay mineralogy of the Waitawhiti rocks.

Sample	Location	Grain size				Clay mineralogy				
		Fine sand % (125 μm < x < 250 μm)	Very fine sand % (63 μm < x < 125 μm)	Silts % (2 μm < x < 63 μm)	Clay % (x < 4 μm)	Smectite %	Illite %	Kaolinite %	C0hlorite %	Interstratified %
07ANN20	Unit B 1, below the western slide		11.51	87.28	8.28	59.21	15.01	9.02	9.72	7.03
07ANN21	Unit B 1, base of the western slide			98.43	**13.57**	**69.49**	10.15	7.55	5.34	7.46
07ANN22	Unit B 1, base of the western slide			98.53	**13.06**	**63.51**	11.85	8.63	6.13	9.88
07ANN23	Unit B 1, base of the western slide		0.10	98.59	**12.31**	**67.87**	12.34	5.10	7.10	7.59
07ANN24	Unit B 1, base of the western slide					**69.85**	11.65	7.74	6.23	4.54
07ANN30	Unit B 2, base of the central slide			96.82	**18.80**	59.43	15.98	10.52	7.88	6.20
07ANN33	Unit B 2, below the northern slide		5.45	93.82	6.74	35.84	28.41	4.83	16.42	14.51
07ANN34	Unit B 2, below the northern slide		5.12	93.88	7.50	62.86	13.33	6.07	8.34	9.40
08WAI05	Unit B 2, below the southeastern slide			98.92	11.64	**64.33**	12.70	3.52	10.48	8.96
08WAI06	Unit B 2, below the southeastern slide	4.96	44.94	49.39	3.81	50.66	16.63	6.79	6.93	18.99
08WAIT	Unit B 2, below the southeastern slide		10.09	89.17	5.82	**69.30**	8.43	18.09	0.00	4.17
07ANN43	Unit B 2, southeastern slide		0.50	97.90	**12.95**	**75.80**	9.24	4.26	4.09	6.62
08WAI02	Unit C, central slide		6.86	92.82	4.98	50.45	17.71	5.68	3.81	22.35
08WAI07	Unit C, northern slide		23.65	75.88	4.08	**64.10**	12.50	4.28	9.93	9.19
08WAI08	Unit C, northern slide		22.61	76.74	5.10	15.55	37.29	20.03	25.03	2.11

x: relative fraction in the sample volume.
Bold data show specific high clay content and high smectite proportion in the possible décollement layers of the slides.

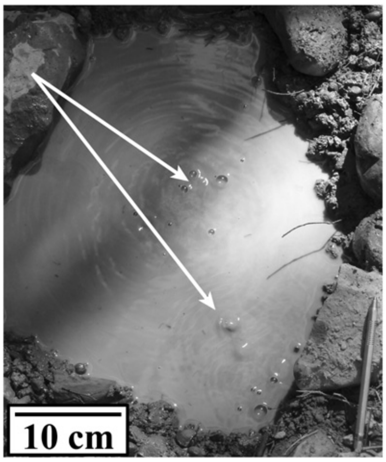

Fig. 6. Example of gas seep discovered in the study area, evidenced here by bubbling water (white arrows) along a stream. See locations in Fig. 3.

for each type of rocks with increasing relative humidity. The strength of water-saturated sandstones dropped tenfold. We could not conduct this kind of water-saturated test on siltstones because samples immediately lost all strength and cohesion once saturated.

Anyhow, these tests indicate that siltstone and sandstone layers, especially when they are saturated with water, have a very low resistance to applied forces and stresses.

4.4. Detailed individual structure of the Waitawhiti landslides

4.4.1. Western Waitawhiti slide

The western Waitawhiti slide (total area = 620 700 m^2), lies on the western flank of the Tawhero syncline, between a lithologically controlled dip slope to the west, and the Woody Gully stream to the east (Figs. 3 and 8a). The surface gradient of the sliding zone is low (~5°), with only a 100-m differential in elevation between the main scarp area and the distal downslope edge (Fig. 8a). In stable areas, strata dips vary from 27° to 10° eastward between the upslope and downslope areas, respectively (western flank of the Tawhero syncline, Figs. 3 and 5).

Fresh, meter-high scarps are found in the upslope western area. A 20 m-high scarp forms the northern main scarp (Fig. 8a). Metric fresh scarps develop upslope of this one (Fig. 8a), suggesting ongoing retrogressing deformation.

The body of the slide has a hummocky morphology (Fig. 8). Sliding blocks can reach 10 m (Fig. 8b), and depressions in between blocks have a short wavelength (about 10 m). Fine-grained sandstone rocks form the “mounds” sliding on siltstone layers of Unit B1 (Fig. 9a). Normal faults, trending perpendicular (NS) to the sliding direction, affect some of the rafted blocks (Fig. 8a), evidencing several phases of eastward gravitational deformation. The direction and dip of the bedding in the blocks could only be measured reliably at one site. The low value of the dip (10°E) indicates that deformation has caused little to no rotation.

The Woody Gully stream has incised about 20 m into the series downslope of the western Waitawhiti slide. In the stream bed, a particular clay-rich siltstone layer crops out (Fig. 9 and Table 1) and is believed to be the *décollement* layer of the slide (see discussion below). All sandstone units overlying this particular layer are affected by normal faults (Fig. 9b), recording extensional deformation in the distal part of the slide. These faults are oriented N169 and dip 32° to the east. Slickensides indicate an N055°E direction of slip. Across the stream, smaller slides are present. We do not discuss these slides in details because of poor outcropping conditions.

In summary, this slide comprises a near-horizontal surface slope and is probably activated by river incision and outcropping of a critical, smectite-rich stratigraphic horizon (Fig. 9 and Table 1). The minor rotations of the blocks, as well as their very disconnected morphology suggest ongoing lateral spreading or translational sliding processes. Spreading affects originally gently tilted lithological units. No accumulation zone or compressional deformations at the downslope edge of the slide could be observed. Instead, extensional deformations have been evidenced close to the river bed (Fig. 9b). This seems consistent with a regular removal of distal sliding deposits by the river.

4.4.2. Central Waitawhiti slide

The 1.344 km^2 central slide affects an area (average surface slope = 11°) steeper than the western slide (Figs. 3 and 10). The stratigraphic series appears for this slide to be horizontal (core of the Tawhero syncline, Fig. 5). Elevations range from 240 m in the distal badland areas to 420 m at the top of the main scarp (Fig. 10). Here, the sliding direction was southward, parallel to the syncline axis (Fig. 3). The sliding mass lies on stable turbiditic series of Unit B2 (Figs. 5 and 11a). These stable turbidites comprise alternating thick metric fine-grained sandstone units and decimetric layers of weathered siltstones. The central slide is bounded downslope by three merging incised valleys. Knickpoints as high as 15 m (Fig. 11b) were observed at elevations about 280 m (Fig. 3). Upstream of these knickpoints, the amount of incision remains low (Fig. 3).

Sliding blocks, having crests parallel to the main scarp, are well-expressed in the eastern half of the slide. In the western half of the slide, such blocks have been smoothed by intense farming work (Fig. 3). The sliding blocks, slightly tilted, are well-expressed in the vicinity of the main scarp, the largest block being about 50 m high (Fig. 10b). The topography of the downslope part of the slide is very smooth, which suggests intense weathering of the sliding blocks (Fig. 10). Siltstone badlands mark the transition between the body of the slide and the incised valley (Fig. 10a). These badlands are a non-structured melange of massive weathered siltstones from Unit C, with fine-grained sandstone from the top of Unit B2. The *décollement* layer, hidden by the badlands, could not be clearly evidenced in the field, but we suspect its location at or above the knickpoints' elevation (280 m), because stable alternating sandstone and siltstone are present immediately below this elevation (Fig. 11a). Fig. 11c shows a schematic block diagram of the stream longitudinal pattern. The incision is best expressed in the fine-grained sandstone units, forming minor knickpoints, whereas siltstones are less eroded. Valley incision remains deep in the turbiditic series. Interestingly, rocks forming the badlands have particularly high clay contents (18.8%, Table 1). Finally,

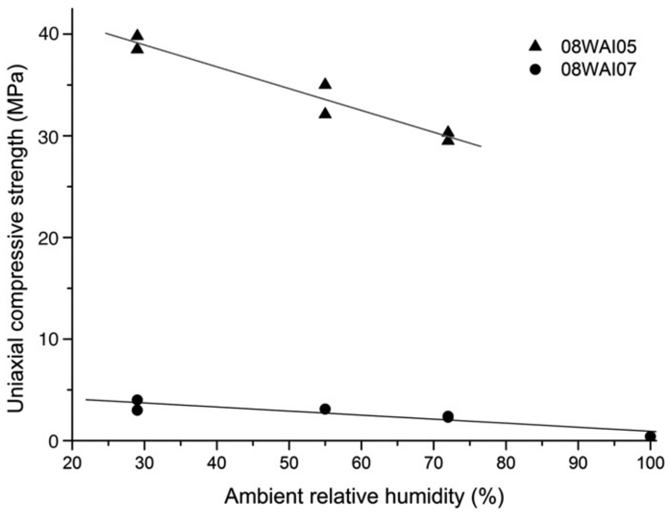

Fig. 7. Graph plotting the uniaxial compressive strength of rocks of the Waitawhiti area with respect to the ambient relative humidity. 08WAI05: siltstone sample; 08WAI07: sandstone sample.

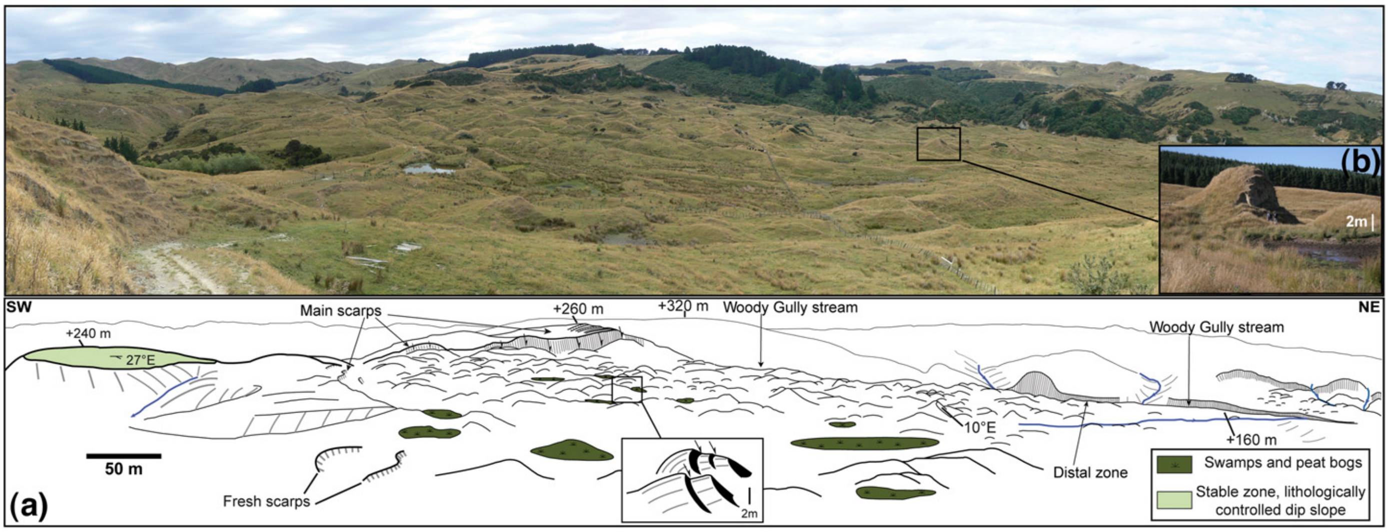

Fig. 8. View of the western slide. (a) Panoramic photograph and line drawing (b) Detail of a sliding block.

metric second-order active scarps found in this area (Fig. 10a) attest for local ongoing advancing activity in the downslope domain of the slide.

In summary, the central slide is globally V-shaped, narrowing greatly downdip. Most likely, the slide was laterally constrained and guided by incision of converging creeks. As in the western slide, no distal compressional structures could be observed. Streams strongly erode the distal parts of the central slide, maintaining continuous removal of sediments and the activity of the slide.

4.4.3. Northern Waitawhiti slide

Fine turbidites and siltstone rocks from the top of Units B2 and C, respectively, slide northward, north of the Waitawhiti road (Figs. 3 and 5). The northern slide is a 1.117 km^2 destabilized body. Its surface slope is about 8°. As observed in the central slide, the northern slide is bounded laterally by shallow-incised valleys and distally by deep-incised valleys. As in the central slide, sliding affects massive weathered siltstones (Fig. 5), making dip measurements and tilt values difficult to assess. Strata appear nearly horizontal in the stable areas surrounding the destabilized body (core of the Tawhero syncline, Fig. 5).

Sliding blocks with crests parallel to the Waitawhiti road are present among a dense drainage network (Fig. 3). Large smoothed blocks form the upslope area, whereas the topography in the downslope area is dominated by smaller-scale hummocks, having a short wavelength (Fig. 3). These hummocks belong to second-order landslides, associated with an advancing activity of the landslide (Fig. 3). Trees tilted southward (Fig. 12a) have recorded the recent activity of the downslope area of the northern slide.

A right-lateral strike-slip fault crosses the slide in its upslope area (Fig. 3). The associated gully offsets range from 10 to 40 m. The vertical normal offset of this fault is thought to be 2 m, on the basis of an observation in a stream incision. The east–northeast orientation of this fault is consistent with main regional fault trends (Fig. 2). However, determining the temporal relationship between the activity of the fault and the sliding onset is very difficult. Indeed, no offset could be observed within the sliding blocks because of their orientation parallel to the fault. Also, the fault does not propagate far outside of the landslide, thus preventing the observation of possible offsets of the fault by sliding. Whether the landslide was prior, late or contemporaneous with the fault activity is not clear.

We observed clear records of compressional deformation in the Waitawhiti complex only at the toe of the northern slide (Fig. 12b). Likely, these compressional structures owe their preservation to the forced meandering of the stream after it was obstructed partly by the sliding event. The compressional structures, which have been removed elsewhere by river activity, include reverse faults having centimetric offsets (Fig. 12b). The faults, initiated in the horizontal series, have been largely tilted during northward sliding (Fig. 12c). A large fold also affects the sliding turbidites (Fig. 12b). Here, sliding turbiditic

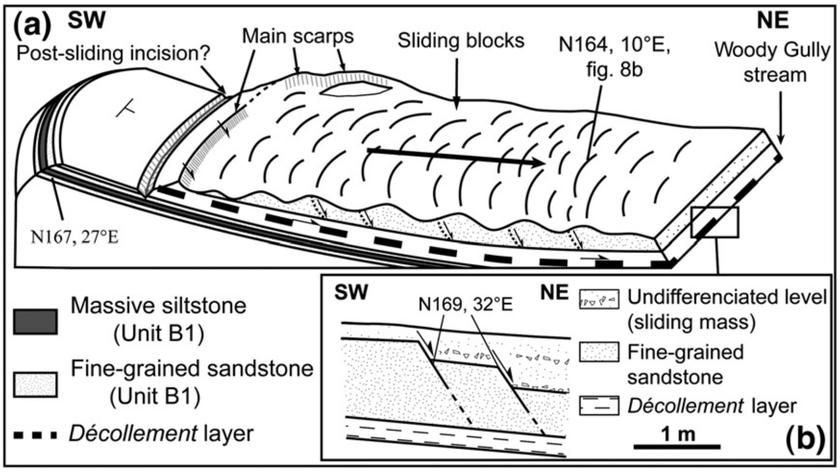

Fig. 9. Schematic interpretation of the western slide. (a) Block diagram. (b) Detailed view of the normal faults affecting the series overlying the inferred *décollement* layer.

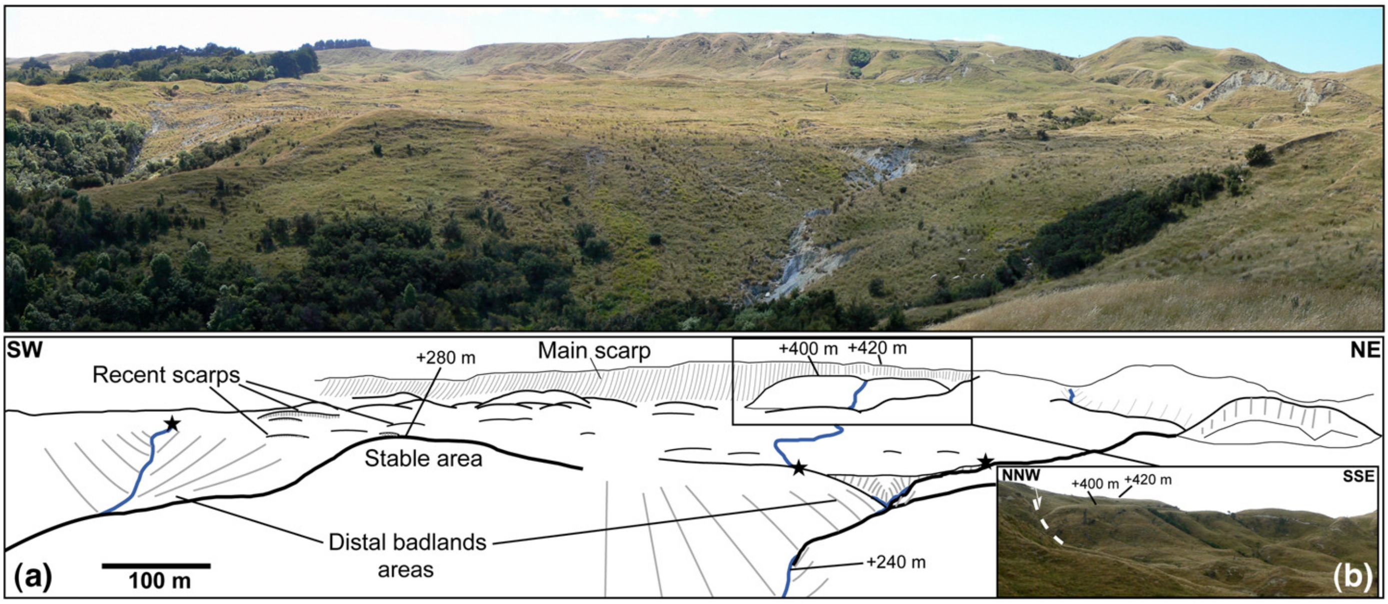

Fig. 10. View of the central slide. (a) Panoramic photograph and line drawing. Stars indicate the location of knickpoints. (b) Detailed view of a sliding block in the upslope domain.

sequences may form the periclinal termination of an anticline. The orientation of the axis of the anticline would then be ~N170. The sliding event is probably responsible for this particular structure.

Finally, we have to emphasize that this slide also displays a triangular planform (Fig. 3). Once again, the presence of a distal incising stream seems to have been a key parameter in the onset of the slide. The presence of an active right-lateral strike-slip fault in the area may have influenced the general morphology of the slide. Likewise, the southeastern slide also is bounded by an NE–SW active fault. These faults may partly control the sliding directions by exposing at the surface critical *décollement* layers, or by creating a structural fabric within the different units.

4.5. Landslide activity

Radiocarbon dating (Table 2) on two pieces of wood sampled in the sliding mass across the western slide, and on a wood fragment trapped in an upslope peat-bog of the central slide, have yielded minimum slide ages of 2857 ± 89 yr cal. BP, 2776 ± 68 yr cal. BP and 1621 ± 80 yr cal. BP, respectively. The northern slide could not be dated. When comparing Quickbird satellite records of 2003 and 2008, we did not find any new large-scale structures within the slides body or in the main scarp areas. However, we could map a metric scarp, retrogressing about 5 m, located upslope the southeastern slide. In the field, fresh scarps and continuously deformed fences correspond to this event (Fig. 13). Tilted trees also show recent activity in the downslope part of the northern slide (Fig. 12a). Ongoing sliding might be seasonal, and strongly influenced by rainfall, as discussed in Section 5.2. Evidence of ongoing activity in the Waitawhiti area is limited to the northern and southeastern slides.

However, the 0.6-m resolution of the satellite images makes it impossible to detect smaller movements. Furthermore, because the polynomial models used for image orthorectification depend on the density of GPS points within the study area, orthorectification remained poorly constrained at the scale of the slides. Indeed, the lack of benchmarks, such as buildings or crossroads, made GPS acquisitions difficult. As a consequence, the three images are not exactly stackable, at least not at a 60-cm horizontal scale.

5. Discussion: Possible determining and triggering factors of landslides

5.1. Fluvial incision

Landsliding in the study area seems closely linked to stream incision. The studied landslides are systematically bounded downstream by

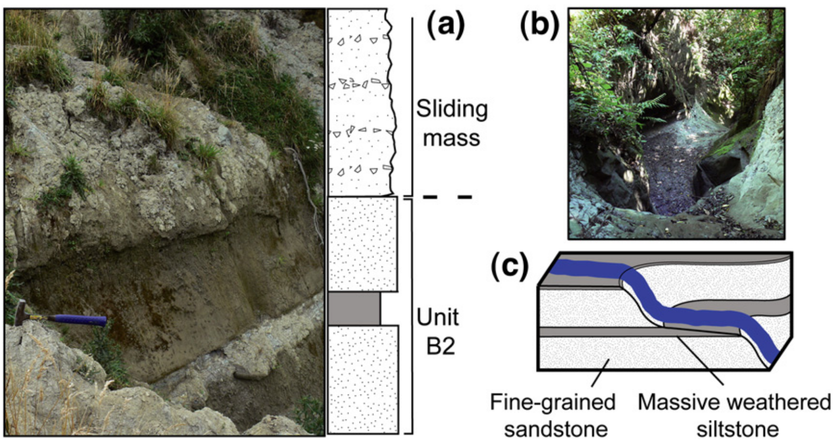

Fig. 11. Details from the central slide. (a) Stable horizontal turbiditic series of Unit B2 overlain by the sliding mass of the central slide. (b) Knickpoints (shot from upstream) in the stream in the downslope domain of the slide. (c) Schematic block diagram showing the preferential location of knickpoints in the streams.

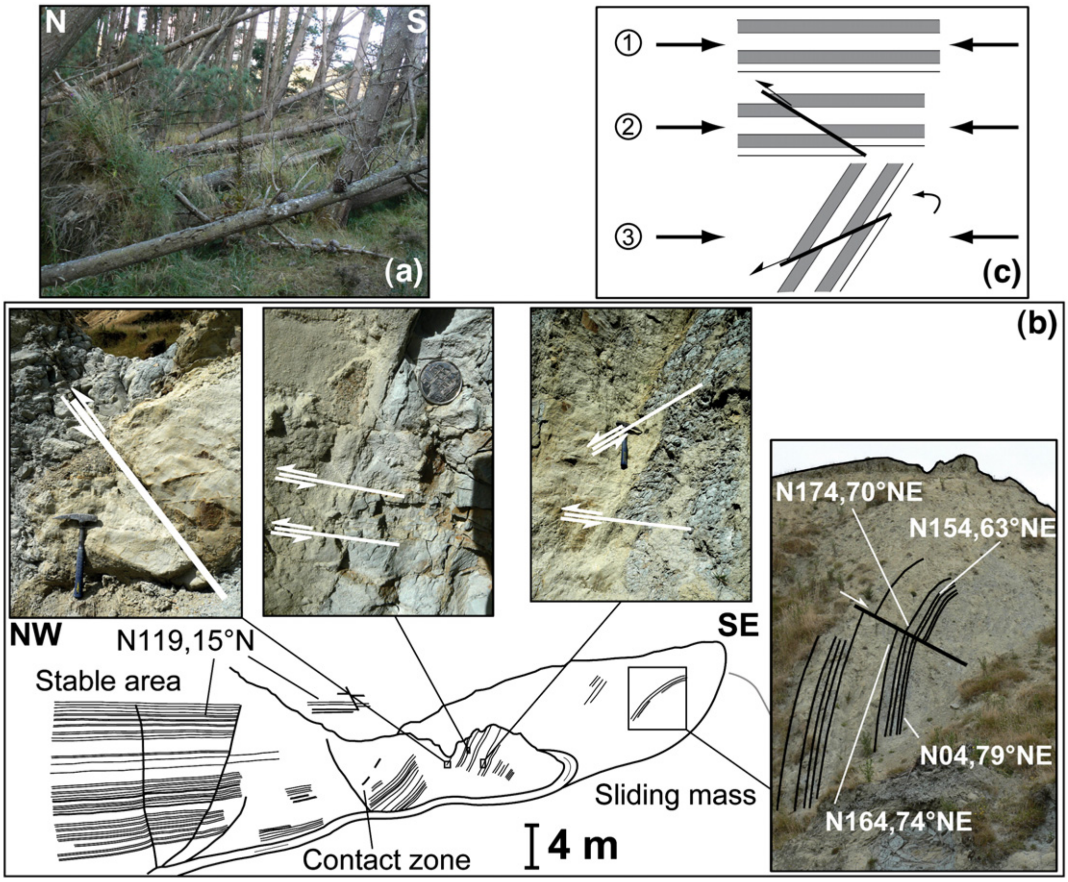

Fig. 12. Details from the downslope part of the northern slide. (a) Photograph of tilted trees. (b) Line drawing of the partly preserved compressional toe of the northern slide and photographs of the associated reverse faults. (c) Sketches illustrating the genesis of tilted reverse faults.

deep-incised valleys exposing low shear-strength *décollement* layers and facilitating horizontal slip of the overlying strata, as described for large rotational slides by Azañon et al. (2005) and for extension in Canyonlands National Park by Schultz-Ela and Walsh (2002). Deep valley incisions cause the continuous removal of the downslope buttresses, thus regularly activating slides through time and preventing the conservation of any compressional distal toes. Laterally, the sliding masses are bounded by less-incised valleys.

In the streams of the study area (tributaries of the Manawatu and Whareama trunk rivers), knickpoint retreat is likely to be the dominant incision process (Figs. 3 and 11). Crosby and Whipple (2006) and Litchfield and Berryman (2006) observed that knickpoint retreat propagating upstream in tributary channels was caused by a postglacial (18 ka) pulse of incision in the trunk rivers of the east coast of the North Island of New Zealand. Litchfield and Berryman (2005, 2006) found that climatic fluctuations (i.e., changes in sediment supply and water flux) have a major influence on the transition between aggradation and incision. They also showed that the effect of the base sea-level changes is restricted to the downstream parts of the rivers (first 50 km from the coast), and that tectonic uplift only enhances the rates of incision, but do not trigger incision. Optimal sediment supply and water flux, coupled with high uplift rates, would then have induced deep postglacial river incisions progressively propagating upstream. The relative ages of the western and central slides are consistent with a mechanism of knickpoint retreat progressing upstream in the Waitawhiti area.

5.2. Rainfall and vegetation

In the Waitawhiti region, poorly-lithified sandstones and highly-fractured siltstones (spheroidal weathering, Sarracino and Prasad, 1989) have high water infiltration rates because of their high porosity and permeability values, probably favouring landslide motion. Lateral shallow stream incision also probably facilitates water infiltration in the slides, thus allowing regular activation of the slides during heavy rainfall. Simple rock-mechanics compression tests (Fig. 7) showed that the strength of the samples decreases when they are saturated with water. Saturated tests could not be conducted on siltstone samples, as pore pressure in small fractures caused these samples to fail before testing. Water flowing within siltstone fractures probably enhances the landslide motion by increasing the pore-fluid pressure and reducing rock strength (Binet et al., 2007), as shown in numerous rainfall-induced landslides (e.g., Rogers and Selby, 1980; Chen et al., 2006). Intense cyclonic rainfall events, such as “Giselle” in 1968 or “Bola” in 1988, are potential triggering factors of large landslides.

Finally, it has been proven that the lack of forest cover as a consequence of massive deforestation also greatly exacerbates the influence of rainfall in triggering slope movements. Reid and Page (2002) showed that sediment loads in rivers in non-forested catchments were up to 10 times those in forested environments. Indeed, deforestation leads to the removal of interconnecting tree-root systems, thereby decreasing the tensional strength of soil (Pearce et al., 1987; Zhang et al., 1993). In the study area, the lack of forest cover may lead to a

Table 2
Radiocarbon ages of wood samples from the western (07ANN25 and 07ANN26) and the central (07ANN56) slides.

Sample	14C age (yr BP)	95.4% (2σ)cal. age (yr BP)	Calibration dataset
07ANN25	2810 ± 35	2857 ± 89	SHCal04 (McCormac et al., 2004)
07ANN26	2680 ± 35	2776 ± 68	
07ANN56	1765 ± 30	1621 ± 80	

Calibrated ages were obtained using the CALIB program (Stuiver and Reimer, 1993).

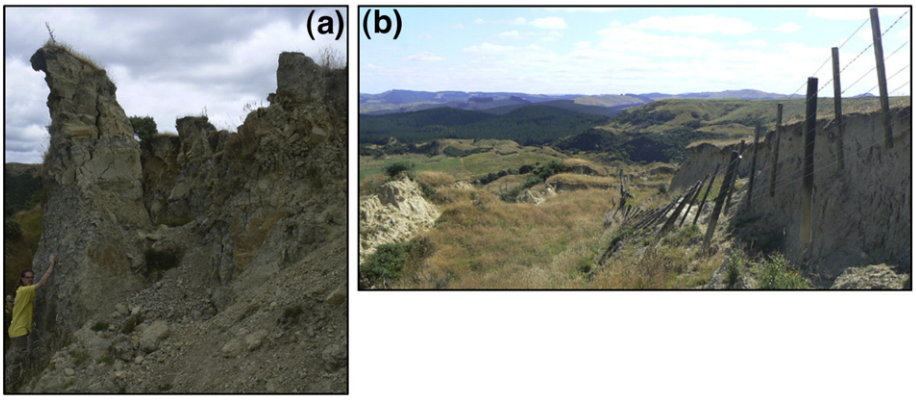

Fig. 13. Records of recent sliding activity in the southeastern slides area. (a) Main scarp and detached block. (b) Suspended fence.

reactivation or an increase in rates of slope movements. Nevertheless, it is important to point out that the loss of forest cover is unlikely to have initially triggered the Waitawhiti landslides because the earlier minimum ages for sliding predate the deforestation. The intensification of erosion caused by deforestation could only induce a positive feedback on channel incision by providing abrasive “tools” necessary for the streams to continue incising, and hence removing distal buttresses, where stream power is large enough to do so.

5.3. Earthquakes and tectonics

Three active faults are associated with the Waitawhiti landslides (Fig. 3). The southeastern slide is clearly bounded laterally by one fault (Fig. 3). We believe that the sliding motion has been localized and guided by the pre-existent fault trace. This right-lateral strike-slip fault could have exposed a critical sliding layer or acted as a guiding fabric. The temporal occurrence of the faults within the western and northern slides is more difficult to constrain: faults do not clearly propagate out of the landslides and do not offset the boundaries of the sliding areas. Conversely, the landslides do not deform fault traces. We however assume that active faults, by creating heterogeneities, may have had an influence on the location and orientation of the Waitawhiti landslides. Tectonic deformation, by inducing preferential structural fabrics and increasing slope gradients, may have favoured and guided sliding.

The presence of three active faults in the study area suggests that the Waitawhiti landslides may have been triggered by the earthquakes associated with these faults, as in other examples in New Zealand (e.g., Lake Waikaremoana landslide; Davies et al., 2006). Indeed, several earthquakes occurred recently at distances less than 45 km from the study area (Pahiatua 1934 earthquake, $M_W = 7.4$; Weber II 1990 earthquake, $M_L = 6.4$), attesting strong regional seismic activity (Schermer et al., 1998, 2004). Moreover, Crozier et al. (1995) showed high landslides density in the vicinity of active fault traces and related landsliding to slip motion on these faults (landslides were particularly numerous at distances less than 2 km from the epicentre).

In addition, considering the impact of tectonics on the Waitawhiti complex, it is important to point out that high uplift rates associated with crustal-scale tectonics probably contribute to increase the hillslopes gradients and rates of fluvial incision, the latter being considered in the study area as a very important triggering and maintaining parameter of slope movements. High Quaternary uplift rates also caused the rapid exhumation of poorly-consolidated rocks, thereby facilitating mass movements.

5.4. Fluids overpressure and lithology

Finally, the presence of thermogenic fluids in the study area may be an additional landslide triggering factor. Indeed, we observed many gas seeps in and around the study area (Figs. 3 and 6), evidencing the upward motion of thermogenic fluids in the region. Gas was found to escape within Unit B1, at stratigraphic levels positioned below the sliding masses. We could observe the seeps only in water-filled streams, but their frequent occurrence in and around the Waitawhiti area led us to think that such fluids, related to active migration of deep thermogenic fluids to the surface, may be widespread across the area. It is known that fluids preferentially rise through fracture zones and permeable layers (Chanier, 1990; Pettinga, 2003). Then, the right-lateral strike-slip faults found in the study area and the poorly-lithified sandstone probably greatly facilitate the gas migration from depth.

In such a context, clay-rich, low-permeability layers that form the base of the western slide (Fig. 9 and Table 1) and potentially the central (Table 1) and northern slides may play a particular role by blocking the ascent of fluids and inducing excess pore-fluid pressures, as described for many examples offshore (Orange et al., 2003; Bayon et al., in press). The mechanical strength of rocks below the low-permeability layers is then strongly reduced, and mass movements of the sedimentary cover can occur. This phenomenon can affect either thin or thick sedimentary covers (e.g., Storegga slide, Huhnerbach and Masson, 2004; Amazon deep-sea fan, Cobbold et al., 2004). In such cases, geotechnical and experimental studies evidenced the secondary role of the basal and surface slope gradients in the triggering of mass movements due to fluids overpressure (surface slope less than 5° for the Gabon slope; Sultan et al., 2004).

However, our results are not specific enough to allow precise quantifications of the deep-origin fluids in the Waitawhiti complex. Fluid overpressure below clay-rich layers is a potential triggering factor for the observed landslides, especially in the case of low-slope-gradient slides, such as the western slide, and low-dipping stratigraphic basal slopes, such as the central and northern slides. The exposure of the *décollement* layer caused by fluvial incision may be an enhancing factor, because of the loss of buttress resistance downslope (Lacoste et al., 2008). Moreover, seismic activity is often associated with pulses in fluid fluxes (e.g., North Anatolian Fault; Géli et al., 2008). Complex interaction among fluid fluxes, seismic cycles (e.g., Miller et al., 1999) and landsliding could be possible in the Waitawhiti area, emplaced on a broad syncline within an active emerged accretionary prism.

6. Conclusions

The Waitawhiti multidirectional landslides involve soft rocks on nearly horizontal strata and are typically V-shaped, bounded by incised valleys. The main destabilizing factor seems to be fluvial incision (controlled by postglacial climatic changes and uplift rates). Incision seems to trigger landsliding by exhuming *décollement* layers and continuously removing distal basal buttresses. The minimum ages of about 2000 yr BP are consistent with a hypothesis of landsliding caused by postglacial downcutting, rather than deforestation, as the initial triggering factor.

Classical triggering factors, such as rainfall and seismic activity, cannot be excluded here. Geotechnical studies show that sandstone and siltstone rocks in the study area have an extremely low strength when they are saturated with water. Regional and active faults mapped in the Waitawhiti area also evidence a strong seismic activity. Earthquakes caused by slip along these faults could have triggered the analysed landslides, as described elsewhere in New Zealand.

Our results also suggest that fluid overpressure, by reducing the effective rock strength of basal low-permeability layers, may have played a significant role in triggering the Waitawhiti landslides. The importance of this process, widely known in submarine slides, is difficult to quantify. Anyway, it is clear that active faulting as well as upward gas migration and trapping in the study area could have led to such overpressures beneath the clay-rich, low-permeability siltstones which acted as *décollement* layers. Gathering quantitative data on the importance of this process would require long-term (several years) monitoring of the sliding activity and fluid fluxes.

Acknowledgments

Acquisition of SPOT5 images presented in this study has been sponsored by the ISIS French program by the CNES (No. ISIS 0411-705). Reviews by Ronald Derose, Mauro Soldati and an anonymous reviewer greatly improved the manuscript. We are grateful to the Richardson and Wright families for providing access to their fields and being so kind and helpful. We also thank Pauline and George Wardle, and their sons, for their kindness and great accommodation at Glenross. We finally acknowledge Jean-Yves Reynaud and Pitaksit Ditbanjong for pleasant and constructive discussions in the field.

Appendix A. Supplementary data

Supplementary data associated with this article can be found, in the online version, at doi:10.1016/j.geomorph.2009.03.001.

References

Azañon, J.M., Azor, A., Vicente Pérez-Peña, J., Carrillo, J.M., 2005. Late Quaternary large-scale rotational slides induced by river incision: the Arroyo de Gor area (Guadix basin, SE Spain). Geomorphology 69, 152–168.
Bailleul, J., 2005. Dynamique sédimentaire et structurale des bassins perchés sur les prismes de subduction, l'exemple du prisme Hikurangi, Nouvelle-Zélande. Thèse de doctorat de l'Université des Sciences et Technologies de Lille, 292 pp. (in French).
Bailleul, J., Robin, C., Chanier, F., Guillocheau, F., Field, B., Ferrière, J., 2007. Turbidite systems in the inner forearc domain of the Hikurangi convergent margin (New Zealand): new constraints on the development of trench–slope basins. Journal of Sedimentary Research 77, 263–283.
Ballance, P.F., 1993. The New Zealand Neogene forearc basins. In: Ballance, P.F. (Ed.), South Pacific Sedimentary Basins, Sedimentary Basins of the World 2. Elsevier Sciences Publishers B.V., Amsterdam, pp. 177–193.
Barnes, P.M., Lewis, K.B., 1991. Sheet slides and rotational failures on a convergent margin: the Kidnappers Slide, New Zealand. Sedimentology 38, 205–221.
Bayon, G., Loncke, L., Dupré, S., Caprais, J.-C., Ducassou, E., Duperron, S., Etoubleau, J., Foucher, J.-P., Fouquet, Y., Gontharet, S., Henderson, G.M., Huguen, C., Klaucke, I., Mascle, A., Migeon, S., Olu-Le Roy, K., Ondréas, H., Pierre, C., Sibuet, M., Stadnitskaia, A., Woodside, J.M., in press. Multi-disciplinary investigation of fluid seepage on an unstable margin: the case of the Central Nile deep sea fan. Marine Geology.
Binet, S., Mudry, J., Scavia, C., Campus, S., Bertrand, C., Guglielmi, Y., 2007. In situ characterization of flows in a fractured unstable slope. Geomorphology 86, 193–203.
Bout-Roumazeilles, V., Cortijo, E., Labeyrie, L., Debrabant, P., 1999. Clay mineral evidence of nepheloid layer contribution to the Heinrich layers in the Northwest Atlantic. Palaeogeography, Palaeoclimatology, Palaeoceanography 146, 211–228.
Chanier, F., 1990. Mud volcanoes on the emerged ridge of the Hikurangi accretionary prism, New Zealand; tectonic setting and structural signification. In: Cadet, J.-P., Le Pichon, X. (Eds.), International Conference on Fluids in Subduction Zones and Related Processes, Paris, 5–6 Novembre, p. 99.
Chanier, F., Ferrière, J., Angelier, J., 1999. Extensional deformations across an active margin, relations with subsidence, uplift, and rotations: the Hikurangi subduction, New Zealand. Tectonics 18, 862–876.
Chang, K.-J., Taboada, A., Chan, Y.-C., 2005. Geological and morphological study of the Jiufengershan landslide triggered by the Chi-Chi Taiwan earthquake. Geomorphology 71, 293–309.
Chen, H., Dadson, S., Chi, Y.-G., 2006. Recent rainfall-induced landslides and debris flow in northern Taiwan. Geomorphology 77, 112–125.
Cobbold, P.R., Mourgues, R., Boyd, K., 2004. Mechanism of thin-skinned detachment in the Amazon Fan: assessing the importance of fluid overpressure and hydrocarbon generation. Marine and Petroleum Geology 21, 1013–1025.
Crosby, B.T., Whipple, K.X., 2006. Knickpoint initiation and distribution within fluvial networks: 236 waterfalls in the Waipaoa River, North Island, New Zealand. Geomorphology 82, 16–38.
Crozier, M.J., Deimel, M.S., Simon, J.S., 1995. Investigation of earthquake triggering for deep-seated landslides, Taranaki, New Zealand. Quaternary International 25, 65–73.
Davies, T.R., McSaveney, M.J., Beetham, R.D., 2006. Rapid block glides: slide-surface fragmentation in New Zealand's Waikaremoana landslide. Quarterly Journal of Engineering Geology and Hydrogeology 39, 115–129.
De Mets, C., Gordon, R.G., Argus, D.F., Stein, S., 1994. Effects of recent revisions to the geomagnetic time scale on estimates of current plate motions. Geophysical Research Letters 21, 2191–2194.
England, P., Molnar, P., 1990. Surface uplift, uplift of rocks, and exhumation of rocks. Geology 18, 1173–1177.
Field, B.D., Uruski, C.I., Beu, A.G., Browne, G.H., Crampton, J.S., Funnell, R., Killops, S., Laird, M.G., Mazengarb, C., Morgans, H.E.G., Rait, G.J., Smale, D., Strong, C.P., 1997. Cretaceous–Cenozoic Geology and Petroleum Systems of the East Coast Region, New Zealand. Institute of Geological and Nuclear Sciences Monograph 19, Wellington. 301 pp.
Fitch, T.J., 1972. Plate convergence, transcurrent faults and internal deformation adjacent to southeast Asia and western Pacific. Journal of Geophysical Research 77, 4432–4460.
Francis, D., 1995. Oil and gas seeps of northern and central East Coast Basin. Petroleum Exploration in New Zealand News 44, 21–27.
Géli, L., Henry, P., Zitter, T., Dupré, S., Tryon, M., Çagatay, M.N., Mercier de Lépinay, B., Le Pichon, X., Sengör, A.M.C., Görür, N., Natalin, B., Uçarkus, G., Özeren, S., Volker, D., Gasperini, L., Bourlange, S., 2008. Gas emissions and active tectonics within the submerged section of the North Anatolian Fault zone in the Sea of Marmara. Earth and Planetary Sciences Letters 274, 34–39.
Ghani, M.A., 1978. Late Cenozoic vertical crustal movements in the southern North Island, New Zealand. New Zealand Journal of Geology and Geophysics 21, 117–125.
Hancox, G.T., Perrin, N.D., Dellow, G.D., 1997. Earthquake-induced Landsliding in New Zealand and Implications for MM Intensity and Seismic Hazard Assessment. Client Report 43601B, Institute of Geological and Nuclear Sciences, Wellington, New Zealand, 105 pp.
Henry, P., Le Pichon, X., 1991. Fluid flow along a decollement layer: a model applied to the 16°N section of the Barbados accretionary wedge. Journal of Geophysical Research 96, 6507–6528.
Hovius, N., Stark, C.P., Allen, P.A., 1997. Sediment flux from a mountain belt derived by landslide mapping. Geology 25, 231–234.
Huhnerbach, V., Masson, D.G., 2004. Landslides in the North Atlantic and its adjacent seas: an analysis of their morphology, setting and behaviour. Marine Geology 213, 343–362.
Hull, A.G., 1990. Tectonics of the 1931 Hawke's Bay earthquake. New Zealand Journal of Geology and Geophysics 33, 309–320.
Johnston, M.R., 1975. Sheet N159 and Part Sheet N158, Tinui-Awatoitoi. Geological Map of New Zealand, 1:63 360, Department of Scientific and Industrial Research, Wellington, New Zealand.
Keefer, D.K., 1984. Landslides caused by earthquakes. Geological Society of America Bulletin 95, 406–421.
Kvenvolden, K.A., Pettinga, J.R., 1989. Hydrocarbon gas seeps of the convergent Hikurangi margin, North Island, New Zealand. Marine and Petroleum Geology 6, 2–8.
Lacoste, A., Vendeville, B.C., Loncke, L., 2008. Role of fluid overpressure and river incision on landslides: field work and experimental modelling. Bollettino di Geofisica Teorica e Applicata Special Issue, International Geological Modelling Conference, Florence, 22–24 September, pp. 458–462.
Lang, A., Moya, J., Corominas, J., Schrott, L., Dikau, R., 1999. Classic and new dating methods for assessing the temporal occurrence of mass movements. Geomorphology 30, 33–52.
Lee, J.M., Begg, J.G., 2002. Geology of the Wairarapa area: Institute of Geological and Nuclear Sciences 1:250000 Geological Map 11. Lower Hutt, New Zealand. Institute of Geological and Nuclear Sciences Limited. 1 sheet + 66 p.
Lillie, A.R., 1953. The Geology of the Dannevirke Subdivision. New Zealand Geological Survey Bulletin 46. 156 pp.
Lin, J.-C., Petley, D., Jen, C.H., Koh, A., Hsu, M.-L., 2006. Slope movements in a dynamic environment – a case study of Tachia River, Central Taiwan. Quaternary International 147, 103–112.
Litchfield, N., Berryman, K., 2005. Correlation of fluvial terraces within the Hikurangi Margin, New Zealand: implications for climate and baselevel controls. Geomorphology 68, 291–313.
Litchfield, N., Berryman, K., 2006. Relations between postglacial fluvial incision rates and uplift rates in the North Island, New Zealand. Journal of Geophysical Research 111, F02007.
Loizeau, J.-L., Arbouille, D., Santiago, S., Vernet, J.-P., 1994. Evaluation of a wide range laser diffraction grain size analyser for use with sediments. Sedimentology 41, 353–361.
Louie, J.N., Chavez-Perez, S., Henrys, S., Bannister, S., 2002. Multimode migration of scattered and converted waves for the structure of the Hikurangi slab interface, New Zealand. Tectonophysics 355, 227–246.
McCaffrey, R., Zwick, P., Bock, Y., Prawirodirdjo, L., Genrich, J., Stevens, C.W., Puntodewo, S.S.O., Subarya, C., 2000. Strain partitioning during oblique plate convergence in

northern Sumatra: geodetic and seismologic constraints and numerical modeling. Journal of Geophysical Research 105, 363–376.
McCormac, F.G., Hogg, A.G., Blackwell, P.G., Buck, C.E., Higham, T.F.G., Reimer, P.J., 2004. SHCal04 southern hemisphere calibration 0–11.0 cal kyr BP. Radiocarbon 46, 1087–1092.
Meng, Q.-R., Hu, J.-M., Wang, E., Qu, H.-J., 2006. Late Cenozoic denudation by large magnitude landslides in the eastern edge of Tibetan Plateau. Earth and Planetary Science Letters 243, 252–267.
Miller, S.A., Ben-Zion, Y., Burg, J.-P., 1999. A three-dimensional fluid-controlled earthquake model: behavior and implications. Journal of Geophysical Research 104, 10621–10638.
Neef, G., 1992. Turbidite deposition in five Miocene, bathyal formations along an active plate margin, North Island, New Zealand, with notes on styles of deposition at the margins of east coast bathyal basins. Sedimentary Geology 78, 111–136.
Orange, D.L., Saffer, D., Jeanjean, P., Al-Khafaji, Z., Humphrey, G., Riley, G., 2003. Measurements and modeling of the shallow pore pressure regime at the Sigsbee Escarpment: successful prediction of overpressure and ground-truthing with borehole measurements. The Leading Edge 22, 906–913.
Pearce, A.J., O'Loughlin, C.L., Jackson, R.J., Zhang, X.B., 1987. Reforestation: on-site effects on hydrology and erosion, eastern Raukumara Range, New Zealand. In: Swanson, R.H., Bernier, P.Y., Woodward, P.D. (Eds.), Forest Hydrology and Watershed Management, vol. 167. International Association of Hydrological Sciences Publication, pp. 489–498.
Pettinga, J.R., 2003. Mud volcano eruption within the emergent accretionary Hikurangi margin, southern Hawke's bay, New Zealand. New Zealand Journal of Geology and Geophysics 46, 107–121.
Pettinga, J.R., 2004. Three-stage massive gravitational collapse of the emergent imbricate frontal wedge, Hikurangi Subduction Zone, New Zealand. New Zealand Journal of Geology and Geophysics 47, 399–414.
Pillans, B., 1986. A Late Quaternary uplift map for North Island, New Zealand. Royal Society of New Zealand Bulletin 24, 409–417.
Reid, L.M., Page, M.J., 2002. Magnitude and frequency of landsliding in a large New Zealand catchment. Geomorphology 49, 71–88.
Rodgers, D.W., Little, T.A., 2006. World's largest coseismic strike-slip offset: the 1855 rupture of the Wairarapa Fault, New Zealand, and implications for displacement/length scaling of continental earthquakes. Journal of Geophysical Research 111, B12408.
Rogers, N.W., Selby, M.J., 1980. Mechanisms of shallow translational landsliding during summer rainstorms: North Island, New Zealand. Geografiska Annaler. Series A, Physical Geography 62, 11–21.
Sarracino, R., Prasad, G., 1989. Investigation of spheroidal weathering and twinning. GeoJournal 19, 77–83.
Schermer, E.R., Van Dissen, R., Berryman, K.R., 1998. In Search of the Source of the 1934 Pahiatua Earthquake. New Zealand Earthquake Commission Report 97/320. 49 pp.
Schermer, E.R., Van Dissen, R., Berryman, K.R., Kelsey, H.M., Cashman, S.M., 2004. Active faults, paleoseismology and historical fault rupture in Northern Wairarapa, North Island, New Zealand. New Zealand Journal of Geology and Geophysics 47, 101–122.
Schultz-Ela, D.D., Walsh, P., 2002. Modeling of grabens extending above evaporites in Canyonlands National Park, Utah. Journal of Structural Geology 24, 247–275.
Shuzui, H., 2001. Process of slip-surface development and formation of slip-surface clay in landslides in Tertiary volcanic rocks, Japan. Engineering Geology 61, 199–219.
Spörli, K.B., 1980. New Zealand and oblique-slip margins: tectonic development up to and during the Cainozoic. In: Ballance, P.F., Reading, H.G. (Eds.), Sedimentation in Oblique-slip Mobile Zones. Special Publication of the International Association of Sedimentologists. Blackwell Scientific Publications, Oxford, pp. 147–170.
Stuiver, M., Reimer, P.J., 1993. Extended 14C database and revised CALIB radiocarbon calibration program. Radiocarbon 35, 215–230.
Sultan, N., Cochonat, P., Cayocca, F., Bourillet, J.-F., Colliat, J.-L., 2004. Analysis of submarine slumping in the Gabon continental slope. American Association of Petroleum Geologists 88, 781–799.
Yu, G., Wesnousky, S.G., Ekström, G., 1993. Slip partitioning along major plate boundaries. Pure and Applied Geophysics 140, 183–210.
Zhang, X., Phillips, C., Marden, M., 1993. A comparison of earthflow movement mechanisms on forested and grassed slopes, Raukumara Peninsula, North Island, New Zealand. Geomorphology 6, 175–187.